Dalton Transactions

ROYAL SOCIETY OF CHEMISTRY

PAPER

View Article Online
View Journal

Cite this: DOI: 10.1039/d6dt01054g

Optimization of Xantphos-type ligands for highly linear-selective hydroformylation of allyl alcohol and alkenes

Hiroto Sakomizu, †[a] Jooyoung Shim,†[a] Shohei Nishizawa,[b] Shinya Tsukamoto,[c] Yoshishige Okuno,[b] Akina Yoshizawa,[a] Eiji Yamamoto,[a] Akihiro Nakayama[a] and Makoto Tokunaga *[a]

Xantphos-type ligands enabled the highly linear-selective hydroformylation of allyl alcohol and related alkenes under mild conditions with $RhH(CO)(PPh_3)_3$. The product, 4-hydroxybutanal, is widely used as an industrial solvent and polymer precursor, and serves as an industrial intermediate in the production of 1,4-butanediol, γ-butyrolactone, and *N*-methyl-2-pyrrolidone. Six ligands with different combinations of the Xantphos backbone and substituents on the benzene ring were compared. A 3,5-xylyl-substituted ligand displayed particularly high regioselectivity toward linear products. Density functional theory calculations clarified that this preference arises from a lower activation barrier for 1,2-insertion compared to 2,1-insertion.

Received 6th May 2026,
Accepted 6th May 2026

DOI: 10.1039/d6dt01054g

rsc.li/dalton

Introduction

Hydroformylation is one of the most important and large-scale homogeneous catalytic processes. Particularly in the petrochemical industry, even slight improvements in yield or selectivity significantly impact costs and profits, making it a critical challenge. 4-Hydroxybutanal (**2a**) is an industrial intermediate for the production of 1,4-butanediol, γ-butyrolactone (**6a**), and *N*-methyl-2-pyrrolidone, which are widely used as industrial solvents and polymer precursors.[1,2] Various synthetic routes may be used to produce **2a**; notably, the hydroformylation of allyl alcohol (prop-2-en-1-ol, **1a**) offers a direct and atom-economical approach to **2a**. However, this reaction typically suffers from poor regioselectivity, producing significant amounts of **3a** (branched isomer, 3-hydroxy-2-methylpropanal) as a by-product.[3] Because the linear (**2a**) and branched (**3a**) isomers have similar physicochemical properties, the separation of **2a** from mixtures containing **3a** remains a major challenge in large-scale manufacturing.

Catalytic strategies to improve regioselectivity in hydroformylation have been extensively investigated within homogeneous systems, while heterogeneous catalysts have also been explored for terminal alkenes.[4,5] Previous studies using monodentate (*e.g.*, triphenylphosphine (PPh_3))[6] or bidentate phosphines (*e.g.*, 1,4-bis(diphenylphosphino)butane)[7] as ligands in Rh-catalyzed hydroformylation have shown limited linear-to-branched ratios (L/B) for the transformation of **1a**. In 2008, White reported the hydroformylation of **1a** catalyzed by a cyclobutene-based phosphine ligand, which exhibited high product yield and a high L/B ratio (Scheme 1a).[8] More recently, Zhao *et al.* demonstrated that phosphine-stabilized single-atom Rh

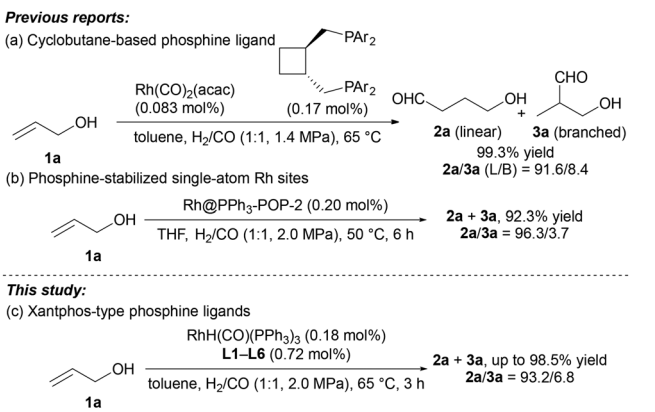

Scheme 1 Rh-catalyzed hydroformylation of **1a**: (a) cyclobutane-based phosphine ligand (White, 2008);[8] (b) phosphine-stabilized single-atom Rh sites (Zhao *et al.*, 2024);[3] and (c) Xantphos-type phosphine ligands developed in this study. L/B = linear-to-branched ratio. Ar = 3,5-$Me_2C_6H_3$.

[a]*Department of Chemistry, Graduate School of Science, Kyushu University, 744 Motooka, Nishi-ku, Fukuoka, 819-0395, Japan. E-mail: mtok@chem.kyushu-univ.jp*
[b]*Research Center for Computational Science and Informatics, Resonac Corporation, 8 Ebisu-cho, Kanagawa-ku, Yokohama, Kanagawa, 221-0024, Japan*
[c]*Kawasaki Plant, Basic Chemicals Business Unit Okawa Development Group, Development Department, Resonac Corporation, 5-1 Okawa-cho, Kawasaki-ku, Kawasaki, Kanagawa, 210-0858, Japan*
† These authors contributed equally to this work.

sites enabled hydroformylation of **1a** with good stability and excellent L/B ratio (Scheme 1b).[3] Computational studies have also suggested that xanthene-based bidentate ligands can improve linear selectivity in the hydroformylation of simple alkenes such as 1-octene (**1c**),[9] although their applicability to more functionalized substrates such as **1a** remains underexplored.

Herein, we report the design and synthesis of electron-rich bidentate phosphine ligands based on the Xantphos scaffold, which markedly enhanced the linear selectivity in the hydroformylation of **1a** and representative alkenes using carbonylhydridotris(triphenylphosphine)rhodium(I) ($RhH(CO)(PPh_3)_3$) as the catalyst precursor (Scheme 1c). Combined experimental and density functional theory (DFT) studies elucidated the origin of the enhanced regioselectivity and provided a mechanistic basis for rational ligand design in Rh-catalyzed hydroformylation.

Results and discussion

Synthesis of L1–L6

The ligand sets used in this study are summarized in Chart 1. Commercially available 4,5-bis(diphenylphosphino)-9,9-dimethylxanthene (Xantphos, **L1**) and 4,6-bis(diphenylphosphino)phenoxazine (Nixantphos, **L2**) were used as benchmarks, together with the reported 6,7-bis(diphenylphosphino) benzo[*k*,*l*]xanthene (Benzoxantphos, **L3**) and *N*-benzyl-4,6-bis (diphenylphosphino)phenoxazine (*N*-benzyl-Nixantphos, **L4**). In addition, we designed and synthesized two novel ligands with sterically demanding di(3,5-dimethylphenyl)phosphino groups: 6,7-bis[di(3,5-dimethylphenyl)phosphino]benzo[*k*,*l*] xanthene (3,5-xylyl-Benzoxantphos, **L5**) and 4,6-bis[di(3,5-dimethylphenyl)phosphino]phenoxazine (3,5-xylyl-Nixantphos, **L6**).

L3 was synthesized in two steps with an overall yield of 39% using a previously reported procedure.[10,11] **L4** was synthesized in 78% yield using a previously reported procedure.[11] These ligands are known to exhibit high linear selectivity in the hydroformylation of 1-octene (**1c**) and styrene (**1e**).[11] **L5** was synthesized in two steps starting from 1-naphthol (Scheme 2). Pd-catalyzed C–C/O bond formation between 1-naphthol and 1,2-dibromobenzene afforded the benzo[*k*,*l*]xanthene framework.[10] Lithiation of 5-bromo-*m*-xylene followed by reaction with dichlorodiethylaminophosphine[12] and subsequent chlorination produced bis(3,5-dimethylphenyl)chlorophosphine,[13] which was coupled with lithiated benzo[*k*,*l*]xanthene to afford **L5** as a pale yellow solid in 25% overall yield.[11] The effects of a remote methyl group are well known, for example, in the asymmetric hydrogenation with modified ligand (*i.e.*, 3,5-xylyl-BINAP).[14] **L6** was synthesized in three steps starting from phenoxazine. Protection of the NH moiety with a *tert*-butyldimethylsilyl group afforded 10-(*tert*-butyldimethylsilyl)phenoxazine.[15] Subsequent lithiation and reaction with bis(3,5-dimethylphenyl)chlorophosphine furnished the corresponding phosphino intermediate. Final desilylation with tetrabutylammonium fluoride afforded **L6** as a pale gray solid in 30% overall yield.[11]

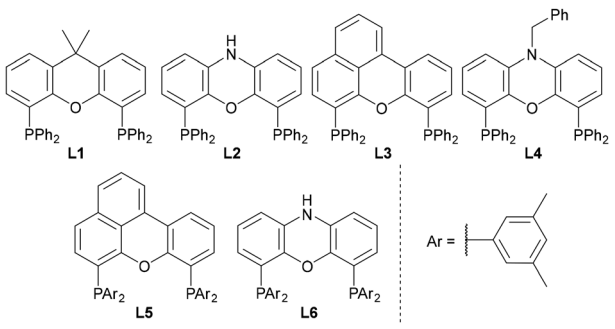

Chart 1 Structures of phosphine ligands **L1** (Xantphos, established), **L2** (Nixantphos, established), **L3** (Benzoxantphos, rarely applied), **L4** (*N*-benzyl-Nixantphos, rarely applied), **L5** (3,5-xylyl-Benzoxantphos, this study), and **L6** (3,5-xylyl-Nixantphos, this study). Ar = 3,5-$Me_2C_6H_3$.

Hydroformylation of allyl alcohol (1a)

The hydroformylation of **1a** was first examined as a benchmark reaction to evaluate the performance of the ligands investigated in this study. The reactions were conducted using $RhH(CO)(PPh_3)_3$ (0.18 mol%) in toluene under syngas (H_2/CO = 1 : 1, 2.0 MPa) at 65 °C for 3 h (see SI for details). The results are summarized in Table 1. The yield of **2a** (linear) was defined as the combined yield of 4-hydroxybutanal and 2-hydroxytetrahydrofuran because these species are in equilibrium in aqueous solution. Benchmark ligands **L1** and **L2** afforded nearly complete conversion of **1a** (>99.8%) and high L/B ratios (93.5/6.5 and 92.9/7.1, respectively); however, only moderate combined yields of **2a** + **3a** (90.6% and 91.7%) were obtained owing to competing β-hydride elimination leading to the formation of propanal (**4a**, 3.8% and 2.1%; entries 1 and 2). Using ligand **L3** slightly improved the combined yield of **2a** + **3a** to 94.3%, while maintaining a high L/B ratio of 93.6/6.4 (entry 3). By contrast, when **L4** was used as the ligand, a performance comparable to that of **L1** and **L2** was noted; **2a** + **3a** was produced in 91.3% yield with an L/B ratio of 92.4/7.6 (entry 4), which was consistent with the benzyl substituent being located relatively distant from the diphenylphosphino moiety, thus exerting only a limited electronic influence. Notably, ligands **L5** and **L6** significantly enhanced hydroformylation performance, affording **2a** + **3a** in 97.0% and 98.5% yields, respectively, while effectively suppressing **4a** formation (1.3–1.5%; entries 5 and 6). Using **L6** as the ligand ensured the highest yield of **2a** + **3a**, with an excellent L/B ratio of 93.2/6.8. These results suggest that sterically demanding and electron-rich diphosphine ligands effectively suppress undesired β-hydride elimination and promote the selective formation of the linear aldehyde. Overall, the observed trends indicate that the ligand environment plays a decisive role in the regioselectivity-determining olefin insertion step, as discussed in detail in the DFT section.

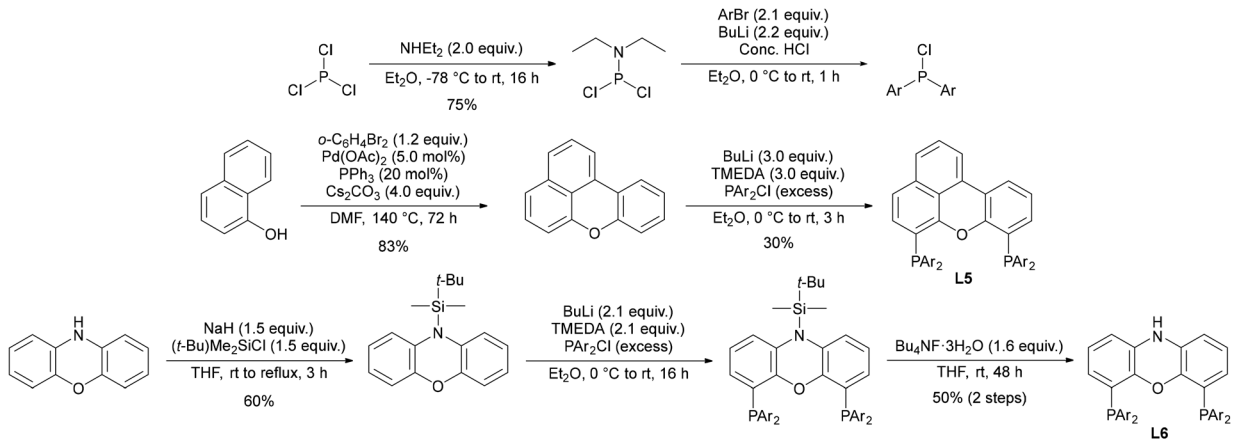

Scheme 2 Synthesis of novel phosphine ligands **L5** and **L6**. Ar = 3,5-$Me_2C_6H_3$.

Table 1 Hydroformylation of **1a** with Rh-phosphine catalysts

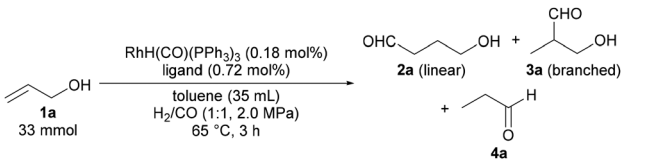

Entry	Ligand	Conv.[a] (%)	Yield[a] (%) 2a[b] + 3a	4a	L/B[c] (2a/3a)
1	**L1**	99.8	90.6	3.8	93.5/6.5
2	**L2**	>99.9	91.7	2.1	92.9/7.1
3[d]	**L3**	>99.9	94.3	1.9	93.6/6.4
4[d]	**L4**	>99.9	91.3	3.4	92.4/7.6
5[d]	**L5**	>99.9	97.0	1.3	93.1/6.9
6	**L6**	>99.9	98.5	1.5	93.2/6.8

[a] Conversions and product yields were determined using high-performance liquid chromatography (HPLC). [b] Yields of **2a** (linear) include the contribution from 2-hydroxytetrahydrofuran. [c] L/B: linear-to-branched ratio. [d] Reaction time: 2 h.

Table 2 Hydroformylation of **1c** with Rh-phosphine catalysts

Entry	Ligand	Ligand (mol%)	Temp. (°C)	Conv.[a] (%)	Yield[a] (%)	L/B[b]
1	**L1**	0.80	65	40	39	98/2
2	PPh_3	0.80	65	>99	>99	75/25
3	**L1**	0.80	80	80	80	98/2
4	**L1**	0.80	90	95	85	98/2
5	**L1**	0.80	100	98	87	98/2
6	**L1**	0.80	110	99	86	97/3
7	**L1**	0.60	65	49	30	98/2
8	**L1**	1.0	65	45	27	98/2
9	**L1**	1.2	65	44	27	98/2
10	**L6**	0.80	90	99	94	98/2

[a] Conversions and product yields (**2c** + **3c**) were determined through gas chromatography (GC) using octanal as the internal standard. [b] L/B: linear-to-branched ratio.

Hydroformylation of other substrates

Hydroformylation is a key industrial process for the large-scale production of bulk chemicals, as exemplified by hydroformylation of propylene to butanal,[16] in which even a small improvement in the yield or selectivity can translate into significant economic benefits. Although this study focused on **1a**, the substrate scope of the hydroformylation reaction was examined after identifying the optimal ligand (**L6**) under the optimized conditions. Seven representative alkenes were investigated to evaluate the generality of this catalytic system, including linear α-olefins (**1b–1d**), aromatic alkenes (**1e** and **1g**), and functionalized allyl derivatives (**1f** and **1h**). Because **1a** exhibits higher reactivity, its hydroformylation proceeded efficiently at a low temperature (65 °C, Table 1). In contrast, hydroformylation of 1-octene (**1c**) under the same conditions gave a low yield of **2c** + **3c** (39%) (Table 2, entry 1). For comparison, when PPh_3 was used as the ligand, **2c** + **3c** was obtained in excellent yield (>99%) under the same conditions, but with a relatively low L/B ratio of 75/25 (entry 2). Increasing the reaction temperature to 80 °C led to an improved yield of **2c** + **3c** (80%) (entry 3). At 90 °C, the reaction proceeded efficiently and afforded a high yield of **2c** + **3c** (85%) (entry 4). Further elevation of the temperature to 100 and 110 °C resulted in only marginal additional enhancement, giving yields of 87% and 86%, respectively (entries 5 and 6). Variation of the ligand loading did not contribute to improved reactivity (entries 7–9); therefore, the conditions shown in entry 4 (90 °C) were selected as the optimized conditions for substrate scope studies.

Under the condition, the yields and selectivities were compared using **L1** and **L6** as ligands (Table 3). Linear α-olefins **1b–1d** underwent hydroformylation to afford the corresponding aldehydes with excellent L/B ratios (>98/<2), and the use of **L6** afforded slightly higher yields (entries 1–3). In the case of styrene (**1e**), where branch selectivity is generally

Table 3 Hydroformylation of various alkenes catalyzed by Rh/**L1** and Rh/**L6**

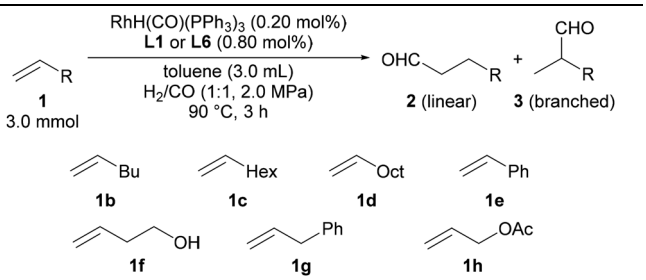

		L1		L6	
Entry	Substrate	Yield[a] (%)	L/B[b]	Yield[a] (%)	L/B[b]
1	**1b**	83	>99/<1	95	>99/<1
2	**1c**	85	98/2	94	98/2
3	**1d**	>99	98/2	>99	98/2
4	**1e**	>99	46/54	>99	51/49
5	**1f**	85	>99/<1	91	>99/<1
6	**1g**	>99	96/4	>99	95/5
7	**1h**	77	85/15	49	97/3

[a] Product yields (**2** + **3**) were determined through GC using octanal or heptanal as an internal standard. [b] L/B: linear-to-branched ratio.

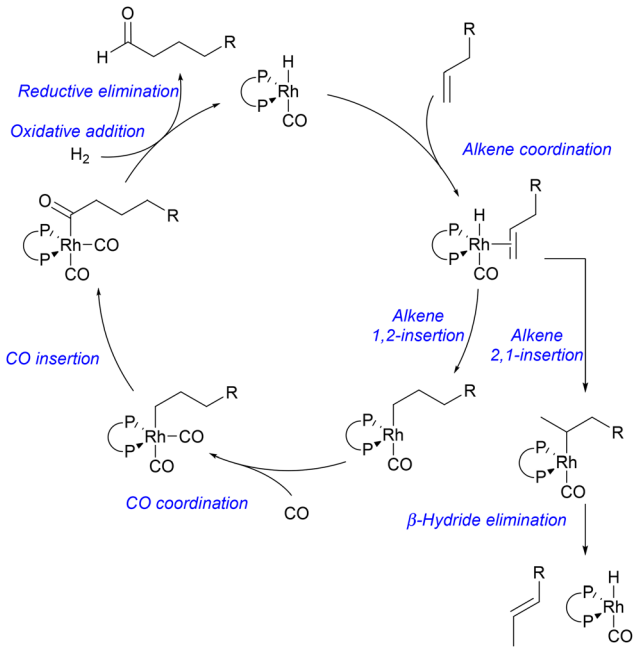

Scheme 3 Widely accepted reaction mechanism for Rh-catalyzed hydroformylation. R represents alkyl group.

observed, **L6** yielded slightly higher L/B ratio (51/49) compared to **L1** (46/54) in quantitative yields (entry 4). The hydroformylation of **1f** proceeded efficiently, followed by intramolecular cyclization to afford the cyclic hemiacetal 2-hydroxytetrahydropyran (**2f**) in high yields (85% and 91% for **L1** and **L6**, respectively) with exclusive linear selectivity (>99/<1), in both cases (entry 5). Allylbenzene (**1g**) was also converted quantitatively (>99%) at high L/B ratios (96/4 and 95/5 for **L1** and **L6**, respectively), indicating that a benzylic substituent does not adversely affect the regioselectivity under these conditions (entry 6). In the case of allyl acetate (**1h**), the results were slightly different from the others (entry 7). **L6** yielded a higher L/B ratio (97/3) than **L1** (85/15). However, the yield was lower when using **L6** (49%) than when using **L1** (77%), presumably due to partial substrate decomposition under the reaction conditions, which may involve β-acetoxy elimination from the corresponding Rh–alkyl intermediate. These results demonstrate that ligand **L6** enables efficient and highly linear-selective hydroformylation across a broad range of terminal alkenes, whereas the reactivity and selectivity of the functionalized substrates are strongly influenced by the nature of the substituents.

Computational mechanistic studies on the hydroformylation

DFT calculations were performed for the hydroformylation of **1a** to gain mechanistic insight into the origin of regioselectivity. As outlined in Scheme 3, the catalytic cycle begins with coordination of the alkene to the Rh center, followed by insertion of the coordinated olefin into the Rh–H bond to form a Rh–alkyl intermediate.[17] Subsequent CO coordination and migratory insertion generate the corresponding Rh–acyl species, which undergo oxidative addition of H_2 and reductive elimination to release the aldehyde and regenerate the Rh–H species. Regioselectivity is determined at the alkene-insertion step: 1,2-insertion affords a linear intermediate, whereas 2,1-insertion forms a branched intermediate. The rate-determining step changes depending on the ligand, CO pressure, and temperature. It is commonly either the alkene coordination/migratory insertion into the Rh–H bond or the oxidative addition of H_2 to the Rh–acyl complex.[18–20] Although not always uniquely defined and can be dependent on the reaction conditions and ligand structures,[21–24] under moderate syngas pressures, Xantphos-type ligands, characterized by a wide bite angle and strongly electron-donating aryl substituents, are expected to render alkene insertion the rate-determining step.[25,26]

In the Xantphos-type ligand system, the steric and electronic nature of the ligand plays a decisive role in controlling the regioselectivity; bulkier electron-donating aryl groups preferentially stabilize the linear-selective transition state over that of the branch pathway. This selective stabilization disfavors the formation of a branched intermediate and rationalizes the experimentally observed enhanced linear selectivity. The relative activation barriers for the two insertion pathways were calculated for ligands **L1–L6** at the ωB97XD/6-31+G* level of theory using Gaussian 16,[27] with the PCM solvation model for toluene (see SI for details). The activation free energy difference, $\Delta\Delta G^{\ddagger}$ = $\Delta G^{\ddagger}$(2,1-insertion) − $\Delta G^{\ddagger}$(1,2-insertion), was used as a descriptor for regioselectivity. The results are summarized in Fig. 1 and 2 (see Table S1 for details), which show the schematic representation of the insertion pathways together with the calculated $\Delta\Delta G^{\ddagger}$ values for each ligand. Benchmark ligands **L1**, **L2**, and **L4** exhibited relatively small

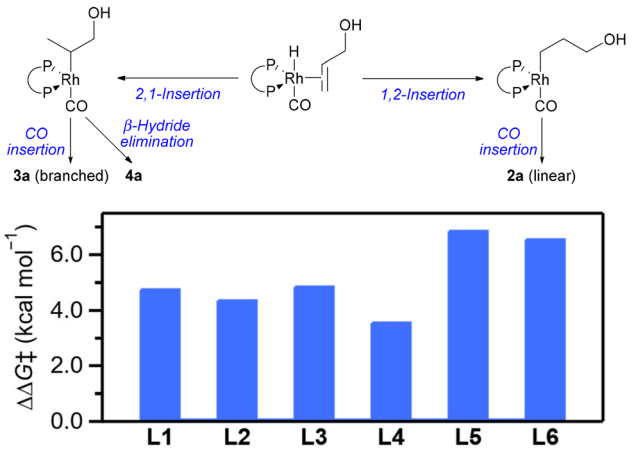

Fig. 1 Schematic representation of the 1,2- and 2,1-insertion pathways of **1a** into the Rh–H bond during hydroformylation (top), and calculated activation free energy differences ($\Delta\Delta G^{\ddagger}$) for ligands **L1**–**L6** (bottom). See SI for computational details.

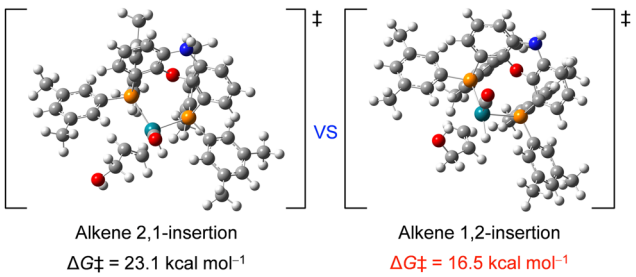

Fig. 2 DFT-calculated transition states for alkene 2,1-insertion (left) and 1,2-insertion (right) into the Rh–H bond with ligand **L6**. The corresponding activation free energies ($\Delta G^{\ddagger}$) are shown. See SI for computational details.

$\Delta\Delta G^{\ddagger}$ values (3.6–4.8 kcal mol^{-1}), in line with their modest experimental regioselectivities. Ligand **L3** displayed a slightly larger $\Delta\Delta G^{\ddagger}$ value (4.9 kcal mol^{-1}), consistent with its improved performance. Notably, ligands **L5** and **L6** exhibited substantially larger $\Delta\Delta G^{\ddagger}$ values (6.9 and 6.6 kcal mol^{-1}, respectively), indicating strong preferential stabilization of the linear-selective transition state.

These computational results correlated well with the experimental trends, where ligands **L5** and **L6** afforded the highest yields of **2a** (linear), although no significant changes in the L/B ratio (**2a**/**3a**) were observed. Notably, the calculated $\Delta\Delta G^{\ddagger}$ values do not account for side processes such as isomerization of **1a** *via* β-hydride elimination to generate **4a** and further transformation; therefore, the experimentally observed L/B ratios (**2a**/**3a**) may deviate from purely kinetic predictions based solely on alkene insertion barriers. While not of synthetic importance, Table S1 displayed the L/B ratios, including byproducts such as propanal (**4a**), propanol (**5a**), and γ-butyrolactone (**6a**), allocated to L/B ratios based on the reaction mechanism. Here, aldehyde **4a** is produced *via* an enol form resulting from the β-hydride elimination of a branched intermediate, and **6a** is the oxidized form of the cyclized linear product **2a**. Since it is unclear whether **5a** was produced *via* the reduction of the branched product **3a** or direct reduction of **1a**, the values for both cases are shown. In either case, the total L/B ratio changed in accordance with the increase or decrease of $\Delta\Delta G^{\ddagger}$, and fairly consistent results were obtained. Importantly, previous studies have shown that increasing the steric bulk of ancillary ligands retards β-hydride elimination;[28] thus, the sterically demanding 3,5-xylyl-substituted ligands **L5** and **L6** are likely to suppress β-hydride elimination, thereby disfavoring the formation of **4a** in this system. This dual effect —preferential stabilization of the 1,2-insertion transition state together with suppression of β-hydride elimination—rationalizes why ligands **L5** and **L6** not only enhance intrinsic regioselectivity at the insertion step but also deliver superior yields of **2a** (linear).

Overall, the DFT calculations support the conclusion that the combined electronic richness and steric bulk of the bis(3,5-xylyl)phosphino substituents enhance linear selectivity by lowering the barrier for 1,2-insertion relative to that of 2,1-insertion while simultaneously suppressing undesired β-hydride elimination, providing a clear mechanistic rationale for the excellent catalytic performance of ligands **L5** and **L6**.

Conclusions

In conclusion, we have developed Xantphos-type ligands that enable the highly linear-selective hydroformylation of allyl alcohol (**1a**) and related alkenes (**1b**–**1h**). In particular, 3,5-xylyl-substituted ligands **L5** and **L6** exhibited exceptional performance, affording **2a** + **3a** in yields of up to 98.5% with an excellent L/B ratio of 93.2/6.8. DFT calculations revealed that the enhanced selectivity originated from a lower activation barrier for 1,2-insertion relative to that for 2,1-insertion. These findings demonstrate that a rational ligand design based on electronic and steric considerations is an effective approach for achieving high linear selectivity in Rh-catalyzed hydroformylation. Furthermore, the introduction of additional electron-donating substituents at the 4-position of the aryl groups may offer a promising strategy to further enhance catalytic performance.

Author contributions

Hiroto Sakomizu, data curation, investigation, validation, visualization, writing; Jooyoung Shim, data curation, investigation; Shohei Nishizawa, conceptualization, formal analysis, methodology, software; Shinya Tsukamoto, conceptualization, data curation, investigation, methodology; Yoshishige Okuno, supervision; Akina Yoshizawa, writing – review & editing; Eiji Yamamoto, writing – review & editing; Akihiro Nakayama, writing – review & editing; Makoto Tokunaga, supervision, writing – review & editing.

Conflicts of interest

There are no conflicts to declare.

Data availability

The data supporting this article have been included as part of the supplementary information (SI). Supplementary information: experimental procedures, DFT studies, and spectroscopic data. See DOI: https://doi.org/10.1039/d6dt01054g.

Acknowledgements

We thank the Service Center of the Elementary Analysis of Organic Compounds, Faculty of Science, Kyushu University, for elemental analyses and the Evaluation Center of Materials Properties and Function, Institute for Materials Chemistry and Engineering, Kyushu University, for high-resolution mass spectrometry (HRMS). We also thank Editage (https://www.editage.jp) for its English language editing services.

References

1 F. Zhou, B. Zhang, H. Liu, Z. Wen, K. Wang and G. Chen, *Org. Process Res. Dev.*, 2018, **22**, 504–511.
2 X. Dong, H. Mo and Y. Chen, *Catal. Commun.*, 2023, **177**, 106647.
3 Y. Zhao, X. Zhou, Z. Yang, S. Hasegawa, K. Motokura, Z. Wang, B. Yu, X. Shi, G. Xu, X. Ding and Y. Yang, *Chem. Eng. J.*, 2024, **502**, 157733.
4 X. Liu, M. Haruta and M. Tokunaga, *Chem. Lett.*, 2008, **37**, 1290–1291.
5 X. Liu, B. Hu, K. Fujimoto, M. Haruta and M. Tokunaga, *Appl. Catal., B*, 2009, **92**, 411–421.
6 R. L. Pruett and J. A. Smith, *J. Org. Chem.*, 1969, **34**, 327.
7 T. Noda and M. Oguri, *Japan Patent Publication Number* H06-279345, 1994.
8 D. F. White, WO2008121194, 2008.
9 M. Kumar, R. V. Chaudhari, B. Subramaniam and T. A. Jackson, *Organometallics*, 2015, **34**, 1062–1073.
10 Y. Terao, T. Satoh, M. Miura and M. Nomura, *Bull. Chem. Soc. Jpn.*, 1999, **72**, 2345–2350.
11 L. A. Van der Veen, P. H. Keeven, G. C. Schoemaker, J. N. H. Reek, P. C. J. Kamer, P. W. N. M. van Leeuwen, M. Lutz and A. L. Spek, *Organometallics*, 2000, **19**, 872–883.
12 J. W. Perich and R. B. Johns, *Synthesis*, 1988, 142–144.
13 D. Mueller, L. Guenee and A. Alexakis, *Eur. J. Org. Chem.*, 2013, 6335–6343.
14 T. Ohkuma, M. Koizumi, H. Doucet, T. Pham, M. Kozawa, K. Murata, E. Katayama, T. Yokozawa, T. Ikariya and R. Noyori, *J. Am. Chem. Soc.*, 1998, **120**, 13529–13530.
15 Y. Antonio, P. Barrera, O. Contreras, F. Franco, E. Galeazzi, J. Garcia, R. Greenhouse, A. Guzman, E. Velarde and J. M. Muchowski, *J. Org. Chem.*, 1989, **54**, 2159–2165.
16 B. Zhang, P. D. Fuentes and A. Börner, *ChemTexts*, 2022, **8**, 2.
17 M. Kumar, R. V. Chaudhari, B. Subramaniam and T. A. Jackson, *Organometallics*, 2014, **33**, 4183–4191.
18 A. Jörke, A. Seidel-Morgenstern and C. Hamel, *J. Mol. Catal. A: Chem.*, 2017, **426**, 10–14.
19 V. S. Nair, S. P. Mathew and R. V. Chaudhari, *J. Mol. Catal. A: Chem.*, 1999, **143**, 99–110.
20 P. W. N. M. van Leeuwen, C. P. Casey and G. T. Whiteker, *Rhodium Catalyzed Hydroformylation in Catalysis by Metal Complexes vol. 22*, Springer, 2008, ch. 4.
21 U. Gellrich, T. Koslowski and B. Breit, *Catal. Sci. Technol.*, 2015, **5**, 129–133.
22 P. C. J. Kamer, A. van Rooy, G. C. Schoemaker and P. W. N. M. van Leeuwen, *Coord. Chem. Rev.*, 2004, **248**, 2409–2424.
23 K. Koehnke, R. Bjornsson, W. Leitner and A. J. Vorholt, *Organometallics*, 2024, **43**, 481–494.
24 P. Patel and A. K. Wilson, *Catal. Today*, 2020, **358**, 422–429.
25 E. Zuidema, L. Escorihuela, T. Eichelsheim, J. J. Carbo, C. Bo, P. C. J. Kamer and P. W. N. M. van Leeuwen, *Chem. – Eur. J.*, 2008, **14**, 1843–1853.
26 L. A. Van der Veen, M. D. K. Boele, F. R. Bregman, P. C. J. Kamer, P. W. N. M. van Leeuwen, K. Goubitz, J. Fraanje, H. Schenk and C. Bo, *J. Am. Chem. Soc.*, 1998, **120**, 11616–11626.
27 M. J. Frisch, G. W. Trucks, H. B. Schlegel, G. E. Scuseria, M. A. Robb, J. R. Cheeseman, G. Scalmani, V. Barone, G. A. Petersson, H. Nakatsuji, X. Li, M. Caricato, A. V. Marenich, J. Bloino, B. G. Janesko, R. Gomperts, B. Mennucci, H. P. Hratchian, J. V. Ortiz, A. F. Izmaylov, J. L. Sonnenberg, D. Williams-Young, F. Ding, F. Lipparini, F. Egidi, J. Goings, B. Peng, A. Petrone, T. Henderson, D. Ranasinghe, V. G. Zakrzewski, J. Gao, N. Rega, G. Zheng, W. Liang, M. Hada, M. Ehara, K. Toyota, R. Fukuda, J. Hasegawa, M. Ishida, T. Nakajima, Y. Honda, O. Kitao, H. Nakai, T. Vreven, K. Throssell, J. A. Montgomery Jr., J. E. Peralta, F. Ogliaro, M. J. Bearpark, J. J. Heyd, E. N. Brothers, K. N. Kudin, V. N. Staroverov, T. A. Keith, R. Kobayashi, J. Normand, K. Raghavachari, A. P. Rendell, J. C. Burant, S. S. Iyengar, J. Tomasi, M. Cossi, J. M. Millam, M. Klene, C. Adamo, R. Cammi, J. W. Ochterski, R. L. Martin, K. Morokuma, O. Farkas, J. B. Foresman and D. J. Fox, *Gaussian 16, Revision C.01*, 2016.
28 J. F. Hartwig, S. Richards, D. Baranano and F. Paul, *J. Am. Chem. Soc.*, 1996, **118**, 3626.

